Measurement of Radiation Efficiency of Multiport Antennas With Feeding Network Corrections

Hasan Raza, Jian Yang, *Senior Member, IEEE*, and Ahmed Hussain

***Abstract*—Multiport antennas are widely used and often integrated with active components, such as low noise amplifiers, in antenna systems. It is important to verify and evaluate the radiation efficiency of a multiport antenna before being integrated in the system. When the radiation efficiency of a multiport antenna is measured, a multiport feeding network is always needed in order to provide the same antenna excitation as it is during its operation after being integrated in the system. This letter addresses how to measure the radiation efficiency of a multiport antenna excluding the losses in the feeding network used for the measurement, particularly when the impedance match between the antenna and the feeding network is not perfect. A rigorous feeding network correction approach is introduced by using measurement data of the radiation efficiency of the whole antenna with feeding network and the S-matrices of both the feeding network and the antenna. As an example of this approach, the radiation efficiency of a multiport Eleven antenna has been determined and verified against the simulated results.**

***Index Terms*—Eleven antenna, measurement, multiport antenna, radiation efficiency, reverberation chamber.**

I. Introduction

MULTIPORT antennas have been used in many applications for many years, such as in phased array antennas and multiple-input–multiple-output (MIMO) antennas [1]–[3].

With the development of integrated circuit technologies, multiport antennas are more and more integrated with amplifiers, phase shifters, and other devices to have compact, low-loss, and multifunctional antenna systems. The cryogenic Eleven feed system [4]–[8], developed for future radio telescopes, is one of the examples of such systems. There are also other multiport antenna systems as candidates for future radio telescopes, such as the improved quadruple-ridged flared horn [9], the sinuous antenna [10], and the quasi self-complementary antenna [11].

It is often required, particularly for integrated antenna systems in radio telescopes, that the radiation efficiency of a multiport antenna, excluding the losses in the feeding network, should be measured before being integrated in the system.

The radiation efficiency of a multiport antenna $e_{\mathrm{rad\_ANT}}$ consists of two factors: the ohmic losses in the antenna itself and the so-called decoupling efficiency that accounts for power returned to nonexcited ports, as defined in [12] (note that $e_{\mathrm{rad\_ANT}}$ here corresponds to $\varepsilon_{\mathrm{totrad}}$ in [12]). Both factors depend on the excitations provided by feeding networks. Different excitations lead to different values of these two factors, therefore different radiation efficiency, for the same antenna. A feeding network that can provide the same excitation as in the final system is therefore needed for the test purpose. However, the test feeding network is often built up of commercially available components in order to reduce the development cost. The losses in the test feeding network could be large, and the impedance match between the antenna and the test feeding network could be far from the perfect case. Thus, it is not a trivial task to obtain the radiation efficiency of a multiport antenna excluding the losses in feeding network.

We present here a rigorous feeding network correction approach for obtaining the radiation efficiency of a multiport antenna. This method uses measurement data of the total radiation efficiency of a multiport antenna with a multiport feeding network, the S-matrices of the feeding network and the antenna, to calibrate out the losses in the feeding network. As an example, a four-port dual-polarized 2–13-GHz Eleven antenna has been measured to determine the radiation efficiency.

For simplicity, the feeding network in the letter has single-input–multiple-output (SIMO) ports. It should be noted that the method is also valid for MIMO feeding network by a little extension of the formulas.

II. Formulation

Fig. 1 shows the block diagram of a general multiport antenna with a multiport feeding network. By multiport antenna, we refer to the multiport antenna without feeding network in this letter. The total radiation efficiency of the whole antenna system with the feeding network $e_{\mathrm{tot\_ANTFN}}$ is defined as

$$e_{\mathrm{tot\_ANTFN}} = \frac{P_{\mathrm{rad}}}{|a_1|^2} \tag{1}$$

where P_{rad} is the total radiated power from the antenna and $|a_1|^2$ is the input power.

The radiation efficiency $e_{\mathrm{rad\_ANT}}$ of the multiport antenna can be expressed as

$$e_{\mathrm{rad\_ANT}} = \frac{P_{\mathrm{rad}}}{\sum\limits_{k=n+2}^{2n+1}\left(|a_k|^2 - |b_k|^2\right)} \tag{2}$$

which measures both the ohmic losses and the decoupling efficiency to nonexcited ports in the multiport antenna.

Manuscript received October 31, 2011; revised December 15, 2011; accepted December 20, 2011. Date of publication January 02, 2012; date of current version March 19, 2012. This work was supported by the Swedish Foundation for Strategic Research (SSF) within the Strategic Research Center CHARMANT and Pakistan's NESCOM scholarship program.

The authors are with the Department of Signals and Systems, Chalmers University of Technology, Gothenburg 41296, Sweden (e-mail: hasan.raza@chalmers.se; jian.yang@chalmers.se; ahmed.hussain@chalmers.se).

Color versions of one or more of the figures in this letter are available online at http://ieeexplore.ieee.org.

Digital Object Identifier 10.1109/LAWP.2011.2182594

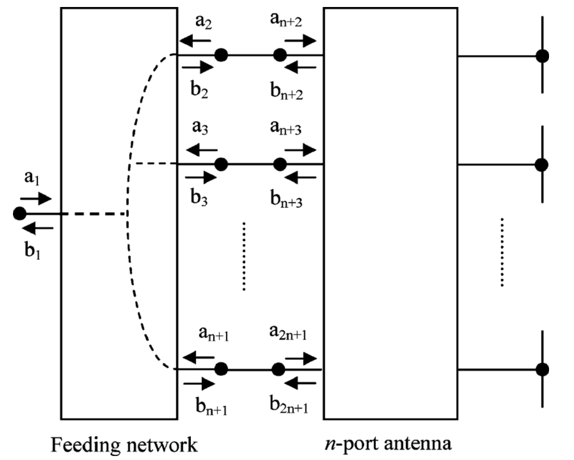

Fig. 1. Block diagram of the configuration of an n-port antenna with its feeding network.

The multiport feeding network can be expressed by the following $\boldsymbol{S}$-matrix

$$\begin{bmatrix} \boldsymbol{b}_{\mathrm{I}} \\ \boldsymbol{b}_{\mathrm{II}} \end{bmatrix} = \begin{bmatrix} \boldsymbol{S}_{\mathrm{I,I}} & \boldsymbol{S}_{\mathrm{I,II}} \\ \boldsymbol{S}_{\mathrm{II,I}} & \boldsymbol{S}_{\mathrm{II,II}} \end{bmatrix} \begin{bmatrix} \boldsymbol{a}_{\mathrm{I}} \\ \boldsymbol{a}_{\mathrm{II}} \end{bmatrix} \tag{3}$$

where

$$\begin{aligned} &\boldsymbol{b}_{\mathrm{I}} = [b_1],\ \boldsymbol{a}_{\mathrm{I}} = [a_1] \quad \boldsymbol{b}_{\mathrm{II}} = \begin{bmatrix} b_2 \\ \vdots \\ b_{n+1} \end{bmatrix} \quad \boldsymbol{a}_{\mathrm{II}} = \begin{bmatrix} a_2 \\ \vdots \\ a_{n+1} \end{bmatrix} \\ &\boldsymbol{S}_{\mathrm{I,I}} = [S_{11}] \quad \boldsymbol{S}_{\mathrm{I,II}} = [\,S_{12} \quad \dots \quad S_{1,n+1}\,] \\ &\boldsymbol{S}_{\mathrm{II,I}} = \begin{bmatrix} S_{21} \\ \vdots \\ S_{n+1,1} \end{bmatrix} \quad \boldsymbol{S}_{\mathrm{II,II}} = \begin{bmatrix} S_{22} & \dots & S_{2,n+1} \\ \vdots & \ddots & \vdots \\ S_{n+1,2} & \dots & S_{n+1,n+1} \end{bmatrix} \end{aligned} \tag{4}$$

where S_{ij} is the S-parameter of the feeding network from port j to port i.

Similarly, the multiport antenna can also be expressed by an $\boldsymbol{S}$-matrix as

$$\boldsymbol{b}_{\mathrm{III}} = \boldsymbol{S}_{\mathrm{III}} \boldsymbol{a}_{\mathrm{III}} \tag{5}$$

where

$$\begin{aligned} &\boldsymbol{b}_{\mathrm{III}} = \begin{bmatrix} b_{n+2} \\ \vdots \\ b_{2n+1} \end{bmatrix} \quad \boldsymbol{a}_{\mathrm{III}} = \begin{bmatrix} a_{n+2} \\ \vdots \\ a_{2n+1} \end{bmatrix} \\ &\boldsymbol{S}_{\mathrm{III}} = \begin{bmatrix} S_{n+2,n+2} & \dots & S_{n+2,2n+1} \\ \vdots & \ddots & \vdots \\ S_{2n+1,n+2} & \dots & S_{2n+1,2n+1} \end{bmatrix}. \end{aligned} \tag{6}$$

From Fig. 1, we have

$$\boldsymbol{a}_{\mathrm{II}} = \boldsymbol{b}_{\mathrm{III}} \quad \boldsymbol{b}_{\mathrm{II}} = \boldsymbol{a}_{\mathrm{III}}. \tag{7}$$

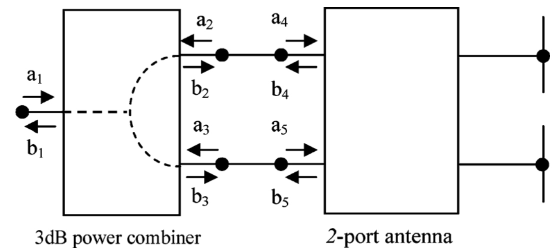

Fig. 2. Block diagram of the configuration of the two-port linearly polarized Eleven antenna of the Balun solution with its feeding network (a 3-dB power combiner).

Therefore, from (3), (5), and (7), we can obtain

$$\boldsymbol{a}_{\mathrm{III}} = (I - \boldsymbol{S}_{\mathrm{II,II}} \boldsymbol{S}_{\mathrm{III}})^{-1} \boldsymbol{S}_{\mathrm{II,I}} \boldsymbol{a}_{\mathrm{I}} \tag{8}$$

where I is the identity matrix. Therefore, $e_{\mathrm{rad\_ANT}}$ can be expressed as

$$\begin{aligned} e_{\mathrm{rad\_ANT}} &= \frac{P_{\mathrm{rad}}}{|\boldsymbol{a}_{\mathrm{III}}|^2 - |\boldsymbol{b}_{\mathrm{III}}|^2} \\ &= \frac{e_{\mathrm{tot\_ANTFN}}}{|(I - \boldsymbol{S}_{\mathrm{II,II}} \boldsymbol{S}_{\mathrm{III}})^{-1} \boldsymbol{S}_{\mathrm{II,I}}|^2 - |\boldsymbol{S}_{\mathrm{III}} (I - \boldsymbol{S}_{\mathrm{II,II}} \boldsymbol{S}_{\mathrm{III}})^{-1} \boldsymbol{S}_{\mathrm{II,I}}|^2}. \end{aligned} \tag{9}$$

Thus, the radiation efficiency $e_{\mathrm{rad\_ANT}}$ of a multiport antenna can be calculated by measured data of the total radiation efficiency $e_{\mathrm{tot\_ANTFN}}$ and $\boldsymbol{S}$-matrices of the feeding network and the multiport antenna.

An approximate method was used in [5] to determine the radiation efficiency, where a perfect impedance matching was assumed between the antenna and the feeding network, i.e., $\boldsymbol{S}_{\mathrm{III}} = 0$, which leads from (9) to

$$e_{\mathrm{rad\_ANT\_approx}} = \frac{e_{\mathrm{tot\_ANTFN}}}{|\boldsymbol{S}_{\mathrm{II,I}}|^2}. \tag{10}$$

The above expression corresponds to the case that the radiation efficiency of a multiport antenna is approximately equal to the total radiation efficiency of the antenna with the feeding network subtracted by the insertion loss of the feeding network.

III. Measurement Example—Radiation Efficiency of the Multiport Eleven Antenna

The Eleven antenna is a compact multiport decade-bandwidth antenna [4]–[8]. The antenna with the passive balun solution [13] is used for verifying the present method. This Eleven antenna can be integrated with two ultrawideband (UWB) passive power combiners and two UWB single-ended low noise amplifiers (LNAs) to make two output ports, one for each polarization. For each polarization, the Eleven antenna is a two-port antenna, and the feeding network is a 3-dB power combiner. The block diagram is shown in Fig. 2.

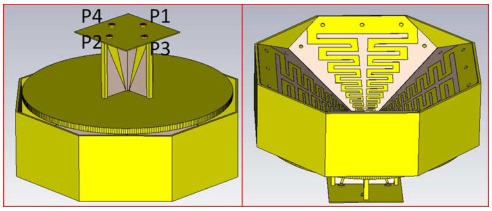

Fig. 3. Simulation model of the four-port dual polarized Eleven antenna.

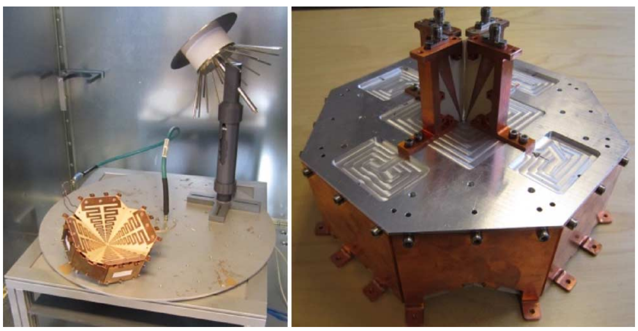

Fig. 4. *(left)* Measurement setup in Bluetest reverberation chamber and *(right)* the four-port dual polarized Eleven antenna with baluns. For one polarization, a two-port Eleven antenna is measured when the other two ports are terminated with loads.

A. Simulation Model

For the sake of the verification, a simulation model of the Eleven feed has been built up in CST MWS [14], as shown in Fig. 3. For the detailed design of the antenna and the baluns, refer to [5] and [13].

The annealed copper ($\sigma = 5.8 \times 10^7$ S/m) is used for all metal parts in the antenna model. The printed circuit boards used for the antenna petals and the baluns are modeled on the substrate of Rogers TMM3 ($\varepsilon_\mathrm{r} = 3.27$, $\mu_\mathrm{r} = 1$, $\tan\delta = 0.002$). All ohmic losses are therefore implemented in this model. Ports P_1 and P_2 are excited simultaneously with the same amplitude and phase, while ports P_3 and P_4 are nonexcited ones, equivalent to being terminated with matched loads. Then, the radiation efficiency of the antenna, without the need of including a feeding network in the model, can be obtained by the simulation in CST.

B. Measurement

The total radiation efficiency $e_{\mathrm{tot\_ANTFN}}$ of the Eleven antenna with the power combiner, including the mismatch factor, was measured in the Bluetest reverberation chamber [15]; see the setup in Fig. 4 (left) and the result (the solid line) in Fig. 7. Note that the remaining two ports of the Eleven antenna for the other polarization are terminated with 50 Ω loads. Therefore, the total radiation efficiency $e_{\mathrm{tot\_ANTFN}}$ includes also the loss leaked to the orthogonal polarization (the decoupling efficiency to nonexcited ports).

The reverberation chamber technology is a fast and economical solution to the so-called over-the-air (OTA) testing for both active and passive antenna devices. It provides accurate and reliable measurements for different antenna characteristics, including the radiation efficiency. Please refer to [16] and [17] for the details. In this letter, the radiation efficiency measurement was performed for the frequency range of 2–8 GHz due to the limitation of the operation frequency band of the chamber.

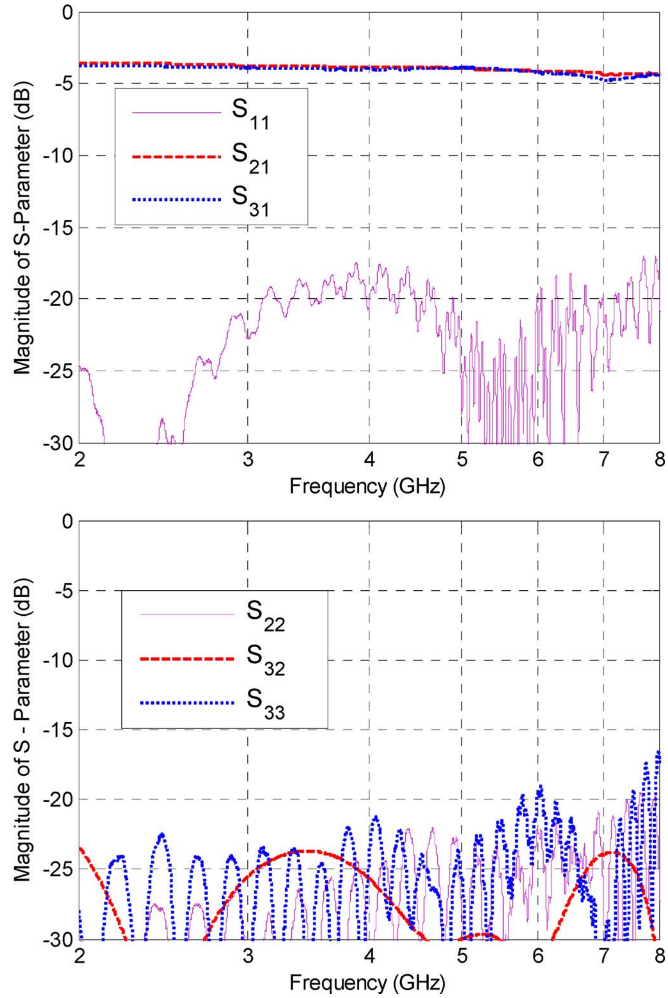

Fig. 5. Magnitude of the measured S-parameters of the feeding network (power combiner).

The $\boldsymbol{S}$-matrixes ($\boldsymbol{S}_{\mathrm{I,I}}$, $\boldsymbol{S}_{\mathrm{I,II}}$, $\boldsymbol{S}_{\mathrm{II,I}}$, $\boldsymbol{S}_{\mathrm{II,II}}$) of the power combiner (the feeding network) and the $\boldsymbol{S}$-matrix ($\boldsymbol{S}_{\mathrm{III}}$) of the two-port linearly polarized Eleven antenna were measured by using a vector network analyzer (Agilent E8363B PNA). All ports of the power combiner and the Eleven antenna are 50-Ω SMA connectors. Figs. 5 and 6 show the measured data.

The radiation efficiency of the Eleven antenna $e_{\mathrm{rad\_ANT}}$ is then calculated based on the measured data by using (9), shown in Fig. 7. The approximate value $e_{\mathrm{rad\_ANT\_approx}}$ defined by (10) is presented here for the sake of comparison. Note that a 50-MHz frequency stirring is used for both the curves. For the details of frequency stirring, refer to [18] and [19]. The simulated radiation efficiency $e_{\mathrm{rad\_sim}}$ of the antenna by using CST is also shown in the figure as the reference for the accuracy evaluation.

From Fig. 6, it can be seen that the matching between the antenna and the feeding network is not always good over the band. However, despite the nonperfect matching, it can be observed in Fig. 7 that the losses introduced by the multiport feeding network can be extracted accurately by using the present method. The radiation efficiency obtained by the present method agrees

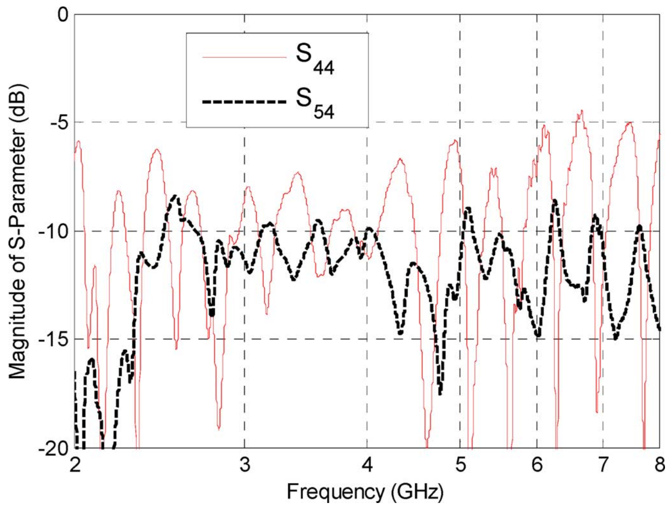

Fig. 6. Magnitudes of the measured S-parameters of the Eleven antenna.

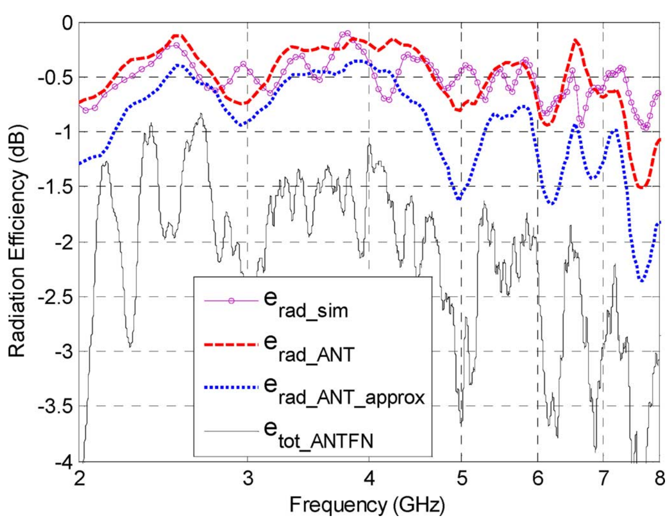

Fig. 7. Radiation efficiency of the Eleven antenna obtained from the measurement and simulation.

very well with the simulated data. Compared to the approximate value $e_{\mathrm{rad\_ANT\_approx}}$, the improvement of the measurement accuracy is between 0.2 and 0.7 dB.

It should be noted that the fluctuation of the measured total radiation efficiency $e_{\mathrm{tot\_ANTFN}}$ of the whole antenna including the feeding network is caused by the characteristic of the reverberation chamber measurement technology, where the number of cavity modes plays a major role for the uncertainty (fluctuation) of the measured data [17].

IV. Conclusion

A rigorous feeding network correction method for determining the radiation efficiency of a multiport antenna based on measurements has been presented. This method removes the losses in the multiport feeding network from the total radiation efficiency, when there are multiple reflections between the antenna and the feeding network due to the mismatch between them. As an example, the measurement results of the radiation efficiency of the Eleven antenna have shown that despite of the impedance mismatch, the radiation efficiency can be obtained accurately by using the present method.

References

[1] R. Mailloux, *Phased Array Antenna Handbook*. Norwood, MA: Artech House, 2005.

[2] D. W. Browne, M. Manteghi, M. P. Fitz, and Y. Rahmat-Samii, “Experiments with compact antenna arrays for MIMO radio communications,” *IEEE Trans. Antennas Propag.*, vol. 54, no. 11, pp. 3239–3250, Nov. 2006.

[3] B. Rembold, “Relation between diagram correlation factors and S-parameters of multiport antenna with arbitrary feeding network,” *Electron. Lett.*, vol. 44, no. 1, pp. 5–7, Jan. 2008.

[4] J. Yang, X. Chen, N. Wadefalk, and P.-S. Kildal, “Design and realization of a linearly polarized eleven feed for 1–10 GHz,” *IEEE Antennas Wireless Propag. Lett.*, vol. 8, pp. 64–68, 2009.

[5] J. Yang, M. Pantaleev, P.-S. Kildal, B. Klein, Y. Karandikar, L. Helldner, N. Wadefalk, and C. Beaudoin, “Cryogenic 2–13 GHz Eleven feed for reflector antennas in future wideband radio telescopes,” *IEEE Trans. Antennas Propag.*, vol. 59, no. 6, pp. 1918–1934, Jun. 2011.

[6] J. Yang, M. Pantaleev, P.-S. Kildal, and L. Helldner, “Compact dual-polarized 1.2 –10 GHz Eleven feed by folding outer elements for large decade-bandwidth radio telescopes,” in *Proc. IEEE Int. Symp. Antennas Propag.*, Spokane, WA, Jul. 3–8, 2011, pp. 843–846.

[7] J. Yin, J. A. Aas, J. Yang, and P.-S. Kildal, “Monopulse tracking performance of multi-port Eleven antenna for use in terminals for satellite communications,” in *Proc. 2nd EuCAP*, Edinburgh, Nov. 11–16, 2007, pp. 1–4.

[8] P.-S. Kildal, R. Olsson, and J. Yang, “Development of three models of the Eleven antenna: A new decade bandwidth high performance feed for reflectors,” in *Proc. 1st EuCAP*, Nice, France, Nov. 6–0, 2006, pp. 1–6.

[9] A. Akgiray, S. Weinreb, and W. Imbriale, “Design and measurements of dual-polarized wideband constant-beamwidth quadruple-ridged flared horn,” in *Proc. IEEE AP-S Int. Symp. Antennas Propag.*, Spokane, WA, Jul. 3–8, 2011, pp. 1135–1138.

[10] R. Gawande and R. Bradley, “Towards an ultra wideband low noise active sinuous feed for next generation radio telescopes,” *IEEE Trans. Antennas Propag.*, vol. 59, no. 6, pp. 1945–1953, Jun. 2011.

[11] G. Cortes-Medellin, “Non-planar quasi-self-complementary ultra-wideband feed antenna,” *IEEE Trans. Antennas Propog.*, vol. 59, no. 6, pp. 1935–1944, Jun. 2011.

[12] M. V. Ivashina, M. N. M. Kehn, P.-S. Kildal, and R. Maaskant, “Decoupling efficiency of a wideband Vivaldi focal plane array feeding a reflector antenna,” *IEEE Trans. Antennas Propag.*, vol. 57, no. 2, pp. 373–382, Feb. 2009.

[13] H. Raza, J. Yang, and M. Pantaleev, “A compact UWB passive balun solution for cryogenic 2–13 GHz Eleven feed for future wideband radio telescopes,” in *Proc. 5th EuCAP*, Rome, Italy, Apr. 11–15, 2011, pp. 921–925.

[14] CST Microwave Studio, 3D EM Simulation Software. Computer Simulation Technology, Framingham, MA, 2011 [Online]. Available: http://www.cst.com

[15] Bluetest Reverberation Test System. Bluetest, Göteborg, Sweden [Online]. Available: http://www.bluetest.se

[16] P.-S. Kildal and K. Rosengren, “Correlation and capacity of MIMO systems and mutual coupling, radiation efficiency and diversity gain of their antennas: Simulations and measurements in reverberation chamber,” *IEEE Commun. Mag.*, vol. 42, no. 12, pp. 102–112, Dec. 2004.

[17] K. Rosengren and P.-S. Kildal, “Radiation efficiency, correlation, diversity gain, and capacity of a six monopole antenna array for a MIMO system: Theory, simulation and measurement in reverberation chamber,” *Proc. IEE, Microw. Antennas Propag.*, vol. 152, no. 1, pp. 7–16, Feb. 2005.

[18] P.-S. Kildal, C. Carlsson, and J. Yang, “Measurement of free-space impedances of small antennas in reverberation chambers,” *Microw. Opt. Technol. Lett.*, vol. 32, no. 2, pp. 112–115, Jan. 2002.

[19] X. Chen and P.-S. Kildal, “Accuracy of antenna input reflection coefficient and mismatch factor measured in reverberation chamber,” in *Proc. 3rd EuCAP*, Berlin, Germany, Mar. 23–27, 2009, pp. 2678–2681.